Non-Sarcomeric Mode of Myosin II Organization in the Fibroblast Lamellum

Alexander B. Verkhovsky*‡ and Gary G. Borisy‡

*A. N. Belozersky Laboratory of Molecular Biology, Moscow State University, Moscow 119899, Russia; and ‡Laboratory of Molecular Biology, University of Wisconsin, Madison, Wisconsin 53706

Abstract. The organization of myosin in the fibroblast lamellum was studied by correlative fluorescence and electron microscopy after a novel procedure to reveal its underlying morphology. An X-rhodamine analog of conventional smooth muscle myosin (myosin II) that colocalized after microinjection with endogenous myosin was used to trace myosin distribution in living fibroblasts. Then, the same cells were examined by EM of platinum replicas. To visualize the structural arrangement of myosin, other cytoskeletal fibrillar structures had to be removed: microtubules were depolymerized by nocodazole treatment of the living cells before injection of myosin; continued nocodazole treatment also induced the intermediate filaments to concentrate near the nucleus, thus removing them from the lamellar region; actin filaments were removed after lysis of the cells by incubation of the cytoskele-tons with recombinant gelsolin. Possible changes in myosin organization caused by this treatment were examined by fluorescence microscopy. No significant differences in myosin distribution patterns between nocodazole-treated and control cells were observed. Cell lysis and depletion of actin also did not induce reorganization of myosin as was shown by direct comparison of myosin distribution in the same cells in the living state and after gelsolin treatment. EM of the well-spread, peripheral regions of actin-depleted cytoskeletons revealed a network of bipolar myosin mini-filaments, contacting each other at their terminal, globular regions. The morphology of this network corresponded well to the myosin distribution observed by fluorescence microscopy. A novel mechanism of cell contraction by folding of the myosin filament network is proposed.

IN addition to its well-established role in striated muscle contraction, myosin is believed to participate in various cell motility phenomena (see Huxley, 1973; Clarke and Spudich, 1977; Adams and Pollard, 1989). Nonmuscle cells contain several types of myosin molecules (for reviews see Korn and Hammer, III, 1988; Pollard et al., 1991; Cheney and Mooseker, 1992) among which there is a species closely related to muscle myosin that is usually referred to as conventional myosin or myosin II. Studies using antibody injection and knockout of the myosin II gene demonstrated that myosin II is essential for certain cell contractility events, such as cleavage furrow formation in cytokinesis (Mabuchi and Okuno, 1977; De Lozanne and Spudich, 1987; Knecht and Loomis, 1987) and the cringing response in interphase Dictyostelium (Fukui et al., 1990). Fibroblast contractility also may depend on myosin II because fibroblasts injected with antibody to this myosin developed extremely elongated shapes (Honer et al., 1988). By gene knockout, myosin II has also been shown to be necessary for *Dictyostelium* cell development (Knecht and Loomis, 1988) and surface receptor capping (Pasternak et al., 1988). Myosin II-deficient *Dictyostelium* amebas exhibited a reduced rate of the cell locomotion (Wessels et al., 1988) which suggested the involvement of myosin II in this process, although other members of the myosin family may also participate.

Several experiments indicated the structural role of myosin II in the organization of the cytoskeleton and the maintenance of cell morphology. Inactivation of the myosin II gene in *Dictyostelium* was reported to result in a weaker organization of the cortical microfilament layer (Fukui et al., 1990). Injection of antibodies to myosin II into living fibroblasts led to cell shape alteration and dissolution of actin stress fibers which was accompanied by an increase rather than decrease in motility (Honer et al., 1988). Experiments using inhibition of myosin II light chain phosphorylation (Lamb et al., 1988), or induction of its dephosphorylation (Fernandez et al., 1990) also suggested a role for this myosin in the organization of stress fibers.

By analogy to muscle, one would expect that if myosin II plays a role in cell motility, some structural organization involving bipolar filaments would be related to its function. This assumption is reinforced by in vitro studies showing that purified cytoplasmic myosin II forms filaments under physiological salt conditions (Niederman and Pollard, 1975; for recent reviews see Korn and Hammer, 1988; Trybus, 1991).

However, myosin filaments have not been extensively identified in nonmuscle cells. As discussed in the literature (Niederman and Pollard, 1975; Mabuchi et al., 1988; Trybus, 1991), this may be due to the fact that in nonmuscle

cells, unlike striated muscle, myosin comprises a comparatively small proportion of the overall cytoskeletal mass; also, small myosin filaments might not be easily distinguishable among the other cytoskeletal structures. The few cases of unambiguous identification of myosin filaments in nonmuscle cells include light microscopic observation in *Dictyostelium* ameba flattened under an agarose sheet (Yumura and Fukui, 1985) and ultrastructural visualization of myosin bipolar filaments in fibroblast cytoskeletal preparations after extraction of actin by gelsolin treatment and loosening of cytoskeletal packing by sonication (Svitkina et al., 1989).

Not much is known about the arrangement of myosin filaments with respect to each other and to the other components of the cultured cell cytoskeleton. The punctate periodic distribution of myosin (Weber and Groeschel-Stewart, 1974; Fujiwara and Pollard, 1976; McKenna et al., 1989) and other muscle-related proteins such as α-actinin and tropomyosin (Lazarides, 1975; Lazarides and Burridge, 1975; Gordon, 1978; for review see Byers et al., 1984) in cultured nonmuscle cells is suggestive of the presence of sarcomeric units similar to the striated muscle ones. To propose a sarcomeric-like myosin arrangement for cultured cells was attractive because it allowed the application of the well-understood contraction mechanism of striated muscle to cytoplasmic contractility. However, the protein arrangement in the cytoskeleton of nonmuscle cells is clearly less regular than in muscle sarcomeres. Unlike muscle, actin in the cytoskeleton is not distributed in a periodic fashion (Goldman et al., 1975) and the polarity of actin filaments does not alternate along filament bundles (Begg et al., 1978). In immunofluorescence studies, individual myosin spots were reported to merge along myosin-containing fibers resulting in a continuous distribution (Fujiwara and Pollard, 1976; Lawson, 1987). On the ultrastructural level, no morphologically clear sarcomeric units have been identified in nonmuscle cells. Indirect evidence of myosin bipolar filaments arranged in such units in fibroblasts was presented by Langanger et al. (1986). In this study, immunogold labeling was used to localize the head and tail portions of myosin molecules within the stress fiber, but the myosin filaments themselves were not visualized.

A non-sarcomeric arrangement of myosin bipolar filaments was observed by Svitkina et al. (1989). Myosin filaments contacted each other at their head-containing ends and formed large continuous assemblies such as chains, bundles, and networks. However, it was not clear whether the extended myosin aggregates were native structures or artifacts induced by the gelsolin treatment and sonication used in the preparative procedure. Another reason to doubt the existence of continuous filament assemblies was that such an idea was hard to reconcile with the well known punctate myosin fluorescence pattern and with the prevailing concept of a sarcomere-like contraction mechanism. Thus, the status of myosin II in nonmuscle cells is not clear at present: neither its specific structural organization nor how that organization accounts for its diverse functions.

To visualize the actual myosin arrangement in cultured fibroblasts and to test for the existence of a non-sarcomeric, continuous mode of myosin filament organization, we performed a correlative imaging study in which the myosin distribution in the living cell was compared with the structural pattern observed by EM.

Materials and Methods

Cell Culture

Swiss 3T3 fibroblasts were grown in HAM's F-10 medium supplemented with 10% fetal bovine serum (Hyclone Labs., Logan, UT) and antibiotics. For microinjection, cells were cultured on glass coverslips mounted with silicon vacuum grease (Dow Corning Corp., Midland, MI) in 35-mm tissue culture dishes. For subsequent location of injected cells, we used coverslips with a finder pattern created by coating with gold through a locator grid for EM (Ted Pella Inc., Redding, CA). Gold coating was performed with an Edwards 12E1 (UK) vacuum evaporator.

Preparation of X-Rhodamine Myosin

The myosin derivatization and injection in high-salt solution was based on the procedure of McKenna et al. (1989). Smooth muscle myosin was prepared from turkey gizzard by the method of Ikebe and Hartshorne (1985), and either used fresh for derivatization or stored under ammonium sulfate. Before derivatization, 100 mM DTT was added to the myosin ammonium sulfate precipitate to a final concentration of 10 mM for complete reduction of thiol groups, precipitate was dissolved in 50 mM Hepes buffer (pH 7.6) containing 0.5 M KCl and 1 mM EDTA and dialyzed overnight against this buffer. Then, the myosin solution (5–10 mg/ml) was rapidly mixed with a 2 mg/ml solution of X-rhodamine maleimide (Research Organics Inc., Cleveland, OH) in DMSO to give a fivefold molar excess of dye over protein and incubated for 2 h on ice. The reaction was stopped by addition of DTT to 10 mM, and free dye was separated by gel filtration on a column equilibrated with injection buffer (5 mM Pipes, pH 7.0, 0.45 M KCl). Protein eluted from the column was stored on ice and used for microinjection within 48 h. Labeled myosin preparations had a protein concentration in the range, 3–6 mg/ml and molar dye/protein ration in the range, 1.5 to 2.8. Electrophoresis of labeled myosin in a 10% polyacrylamide gel by the method of Laemmli (1970) is shown in Fig. 1. As can be seen, most of the dye was associated with the myosin light chains which were widely separated from the heavy chains. Under these electrophoretic conditions, the individual classes of light chain were not resolved from each other.

Microinjection

For microinjection, we selected the cells that retained well-spread, peripheral regions after incubation in nocodazole. Before microinjection, myosin solution was spun at 100,000 g for 10 min to remove particulates. Microinjection was performed at room temperature with a micropipette having a tip diameter of about 1 μm using a Leitz micromanipulator (E. Leitz, Inc., Rockleigh, NJ) and a gas-tight syringe (Hamilton, Reno, NV) as a pressure source. Under standard conditions in the laboratory for microinjection, approximately 5% of the cell volume is injected. After injection, the culture medium was replaced and the cells were returned to the incubator for 2 h to allow for myosin incorporation.

Lysis of the Cells and Extraction of Actin

Extraction of the cells was based on a procedure of Avnur et al. (1983), and performed essentially as described by Verkhovsky et al. (1987) with minor modifications. The cells were rinsed out of culture medium with PBS and lysed with 1% Triton X-100 in a solution containing 50 mM MES-KOH buffer, ph 6.0, 5 mM μgCl₂, 3 mM EGTA, and 4% polyethyleneglycol (M_r-40,000) for 3 min. Lysed cells were washed three times with a solution containing 50 mM MES-KOH, pH 6.3, 0.1 mM CaCl₂, 2 mM μgCl₂, 0.5 mM DTT (buffer A), and incubated in a drop of solution of 0.1–0.2 mg/ml gelsolin NH₂-terminal 45-kD domain (Kwiatkowski et al., 1989) in buffer A for 1 h. Recombinant gelsolin NH₂-terminal domain was a generous gift of Dr. Helen L. Yin (University of Texas Southwestern Medical Center at Dallas, Dallas, TX). It was stored at −70° and dialyzed against buffer A for 2 h shortly before treatment of the cells. After incubation in gelsolin, cells were washed again with buffer A and then observed by light microscopy or (and) fixed and processed for EM.

To test the stability of myosin organization under different conditions, we also performed a separate set of experiments where cells were extracted and treated with gelsolin in PHEM buffer of Schliwa and van Blerkom (1981) with modifications. In this case, extraction of the cells was performed in 60 mM Pipes, 25 mM Hepes, pH 6.9, 2 mM MgCl₂, 2 mM EGTA, 0.5 mM DTT, 0.5% Triton X-100, and 4% polyethyleneglycol (M_r-40,000). Buffer for incubation with gelsolin contained 60 mM Pipes, 25 mM Hepes,
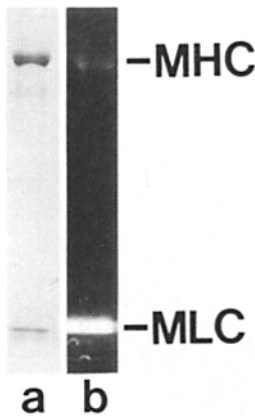
Figure 1. SDS-PAGE of the turkey gizzard myosin preparation used for microinjection in Swiss 3T3 fibroblasts. (a) Coomassie brilliant blue staining of the gel, (b) fluorescence of xrho-myosin. The positions of myosin heavy chain (MHC) and myosin light chains (MLC) are noted.

pH 6.9, 2 mM $MgCl_2$, 0.1 mM $CaCl_2$, and 0.5 mM DTT. 50–100 mM KCl and/or 1 mM ATP were added to both extraction and incubation buffers as indicated in the text.

Fluorescence Microscopy

A microscope (IM 35; Carl Zeiss, Oberkochen, Germany) equipped with a 100 W mercury arc lamp was used for fluorescence microscopy of both living and lysed cells. A SIT camera (Dage-MTI, Inc., Michigan City, NY) was used for searching and focusing, and digital images were acquired with a series 200 CCD camera (Photometrics Ltd., Tucson, AZ) containing a 384 × 576 pixel chip (Thompson CSF TH7882CDA) that was thermoelectrically cooled to −50°C to reduce the dark current noise. Images were digitized to 14-bit depth and stored on WORM drive optical discs (model 3363; IBM Corp., Danbury, CT). An Image-1 (Universal Imaging Corp., Westchester, PA) video processor was used for image processing. During processing, images were scaled to 8-bit depth, background fluorescence intensity values measured in cell-free areas were subtracted from the images and the contrast was linearly enhanced in a way so most of the variation in fluorescence intensity of the image fit into a 256 grey level scale. In some images of living cells, small highly fluorescent regions near the center of the cell were adjusted to slightly exceed the brightest level of the scale, but the dimmest features of the images were always retained within the scale and made clearly visible. Film negatives of the images were obtained from the digital files using a 4,000 line film recorder Matrix PCR (Matrix Instruments Inc., Orangeburg, NY).

Staining of Cytoskeletal Structures

Cytoskeletal actin was stained with bodipy-phalloidin (Molecular Probes, Inc., Eugene, OR); microtubules were visualized with mouse monoclonal anti-β-tubulin antibody (Amersham Corp., Arlington Heights, IL); intermediate filaments were visualized with a mAb of broad specificity (Pruss et al., 1981) generated by a cell line obtained from ATCC (a gift from Dr. C. Simerly, Dept. of Zoology, University of Wisconsin, Madison); affinity purified polyclonal antibody to non-muscle myosin was prepared and used as described earlier (Verkhovsky et al., 1987). The secondary antibodies used were a fluorescein-conjugated anti–mouse IgG, and a fluorescein conjugated anti–rabbit IgG. Before staining for actin microfilaments, myosin, microtubules, and intermediate filaments, lysed cells were fixed with a 4% formaldehyde solution in PBS and washed with PBS. Distribution of injected X-rhodamine myosin (xrho-myosin)[1] in lysed cells was observed without fixation because formaldehyde fixation interfered with the further preparation of the cells for EM and glutaraldehyde fixation created autofluorescence that interfered with myosin imaging.

Electron Microscopy

Platinum replicas were prepared essentially as described by Svitkina et al. (1984). Cytoskeletons were fixed in 2% glutaraldehyde, 0.1% tannic acid solution in 0.1 M sodium-cacodylate buffer, pH 7.2, dehydrated in anhydrous alcohol dried with molecular sieve, critical point–dried following the procedure of Ris (1985) to prevent contamination with traces of water, and coated with platinum and carbon. Replicas were then separated from the

coverslips with the use of hydrofluoric acid, mounted on formvar-coated grids, and observed and photographed with a Phillips 300 transmission electron microscope.

Results

Removal of Microtubules, Intermediate Filaments, and Actin Filaments

To allow the ultrastructural organization of myosin to be made clearly visible by EM, we removed other cytoskeletal structures which interfered with the morphological identification of the myosin filaments. For this purpose, we used a hybrid strategy first to deplete the lamellum of microtubules and intermediate filaments and then to selectively extract the actin, essentially as described previously (Svitkina et al., 1989). Living fibroblasts were treated with nocodazole (500 nM) to depolymerize microtubules (De Brabander et al., 1976). Although microtubule depolymerization occurs quickly, that is, within 30 min (De Brabander et al., 1982), long-term incubation is not deleterious since repolymerization of microtubules occurs rapidly upon washing out the drug. Incubation in nocodazole was continued for 12–24 h because long-term incubation also induces collapse of intermediate filaments from an extended array to a perinuclear mass, thus removing them from the lamellar regions (Goldsman and Knipe, 1972; Geuens et al., 1983; Mittal et al., 1989). The cells were then lysed in detergent and the cytoskeletons treated with gelsolin to remove actin. Indirect immunofluorescence staining with a monoclonal antibody to tubulin or a mAb of broad specificity to intermediate filament proteins confirmed that nocodazole treatment resulted in complete depolymerization of microtubules and concentration of most of the intermediate filaments to the perinuclear region, leaving the cell lamellum essentially free of these structures (data not shown).

The extent of actin extraction by gelsolin treatment was determined by quantitative fluorescence measurement of residual actin stained with bodipy-phalloidin. Cytoskeletons incubated in buffer without gelsolin served as a control. Control cytoskeletons contained well pronounced actin structures brightly stained with phalloidin (Fig. 2 a) whereas gelsolin-treated cytoskeletons exhibited very weak fluorescence, which could be detected only when much longer exposure times or higher digital enhancement of image contrast were used. The predominant fluorescence pattern of the enhanced image of gelsolin-treated cytoskeleton (Fig. 2 b) was diffuse with some weakly fluorescent linear structures which may represent the remnants of stress fibers. The rather bright nuclear and perinuclear fluorescence in these preparations was not due to actin, since it could be detected even without phalloidin staining (not shown). In control cytoskeletons stained with phalloidin, this nonspecific intrinsic fluorescence of the perinuclear region was not visible because of the much brighter actin staining.

To quantitatively estimate the extent of actin removal from the cell periphery, we averaged the mean fluorescence intensity values in rectangular areas embracing peripheral regions of the phalloidin stained control and gelsolin-treated cells ($n \geqslant 20$ for each experiment). The ratio of average intensities (gelsolin treated to control) varied in different experiments from 0.11 ± 0.09 to 0.03 ± 0.02 (mean $\pm$ SD). To determine

---

1. *Abbreviation used in this paper*: X-rhodamine-myosin, xrho-myosin.
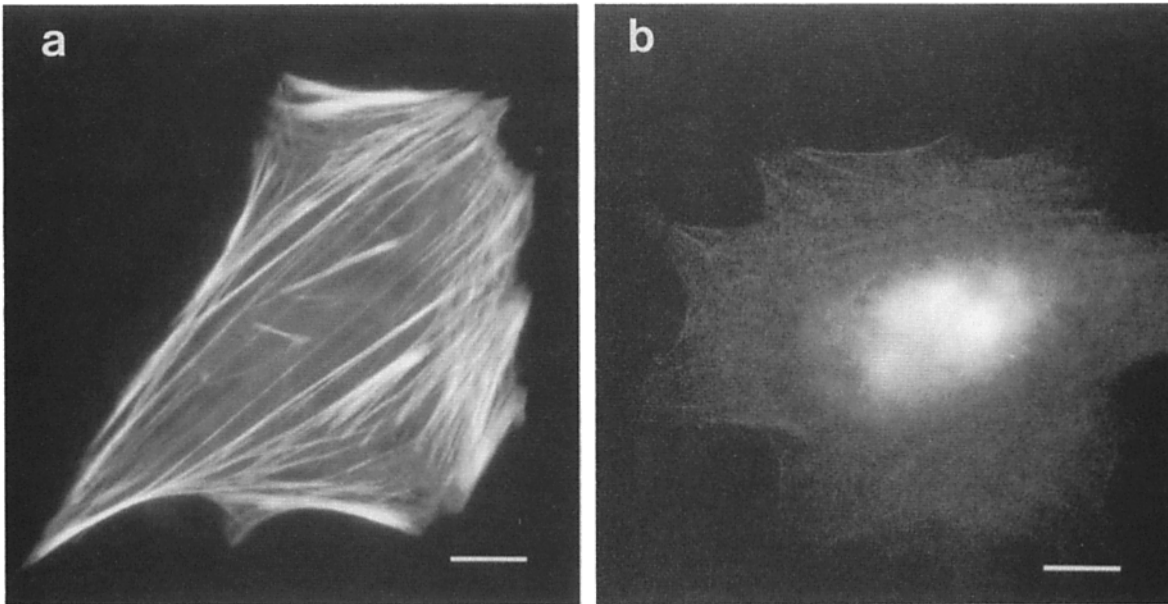
Figure 2. Extraction of actin from fibroblast cytoskeleton by gelsolin treatment. Bodipy-phalloidin staining of cytoskeleton treated with buffer (a) and with 0.2 mg/ml gelsolin NH$_2$-terminal domain (b). Contrast in (b) was digitally enhanced to an extent equivalent to an exposure five times longer than in (a). Bar, 10 μm.

the contribution of fluorescence which was not dependent on staining with phalloidin (background or autofluorescence) and therefore not caused by incomplete actin extraction, two coverslips were simultaneously treated with gelsolin and then one of them was stained with phalloidin while the other was not stained. The average fluorescence intensities in the peripheral regions of stained and unstained cells were similar and equaled 0.03 ± 0.02 and 0.04 ± 0.03 of the fluorescence intensity of the phalloidin-stained control, respectively. Therefore, in the periphery of the cell, as well as in the perinuclear region, at least part (if not all) of the fluorescence intensity observed after gelsolin treatment was not due to actin. Based on these measurements, we estimate that gelsolin treatment removes, on average, ≥90% of cytoskeletal actin, in agreement with conclusions drawn from a previous qualitative study (Verkhovsky et al., 1987).

Incorporation of Xrho-Myosin

As outlined in the previous section, our strategy to visualize myosin for EM included removal of microtubules and intermediate filaments from the cell lamellae by prolonged incubation of living cells with nocodazole. Nocodazole treatment produced some changes in cell morphology which have been described as consequences of microtubule depolymerization (Vasiliev and Gelfand, 1976). Nocodazole-treated cells on average looked less polarized and less spread than cells before treatment. After prolonged incubation in nocodazole many cells exhibited multiple variable-sized nuclei which was an expected result of abortive mitoses. However, many cells retained well-spread lamellae after treatment and these were selected for microinjection of xrho-myosin. To evaluate the normal pattern of myosin incorporation and check if nocodazole treatment altered it, we performed also injection of myosin in control cells not treated with nocodazole. After microinjection, cells were incubated for 2 h to allow for my-

osin incorporation. In the case of nocodazole-treated cells, both injection and subsequent incubation were performed in the continued presence of nocodazole.

Direct fluorescence imaging of living as well as extracted microinjected cells showed that xrho-myosin incorporated into characteristic cytoskeletal structures: stress fibers displaying both punctate and continuous distribution and a networklike arrangement of fine beads in the cell lamellae (Figs. 3, 4, and 5 [inset]). The overall pattern of the incorporation was very similar in control and nocodazole-treated cells (Fig. 3, a and e). The relative abundance of continuous fibrous and punctate beadlike structures was highly variable from cell to cell and between different regions of the same cell. Both nocodazole-treated and control cells exhibited the whole spectrum of this variation. One of the prominent cell types in both control and nocodazole-treated populations showed relatively few continuous fibers in the middle of the cell and extensive networklike arrangement of more or less distinct beads in the peripheral regions (see Figs. 3 e and 5 [inset] for nocodazole-treated and Fig. 3 a for control cell). Other cells showed more abundant continuous or slightly punctate fibers (see Fig. 4 for nocodazole-treated cell; not shown for control cell) mixed with some beadlike structures in lamellar regions (Fig. 4, f and g). Under closer examination beadlike punctate structures usually did not seem strictly discontinuous: spaces between beads exhibited a level of fluorescence above background although lower than within the beads themselves. On the other hand, seemingly continuous fibers also often exhibited variations of fluorescence intensity along their length. Therefore, there seemed to be no sharp distinction between so-called continuous fibers and beadlike structures. Myosin-containing beads usually were rather variably sized and spaced, so no clear long-range periodicity in their distribution was observed. This pattern of myosin incorporation is actually consistent with the images obtained in earlier studies on myosin dis-
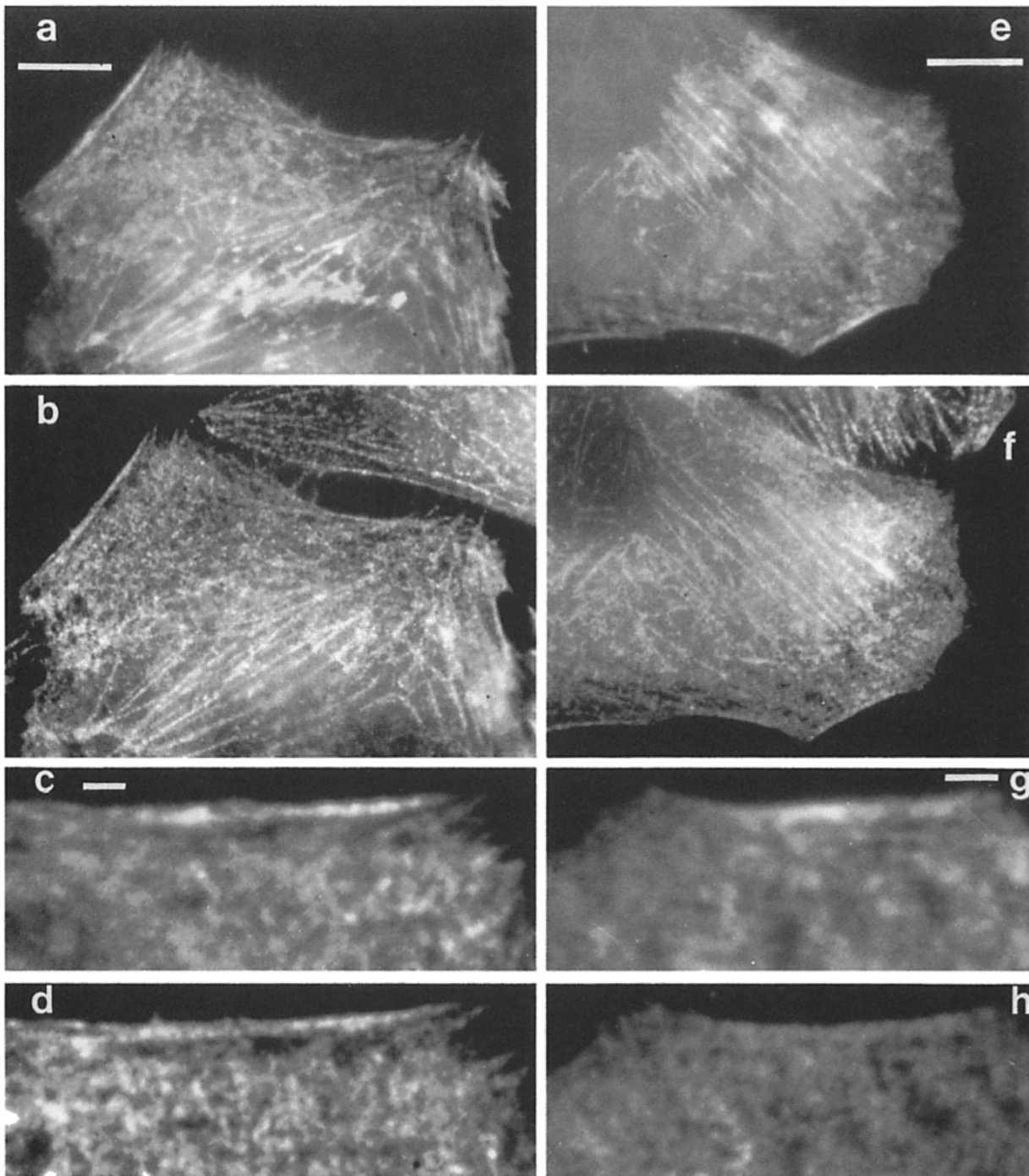
Figure 3. Comparison of injected xrho-myosin fluorescence in living cells (*a, c, e,* and *g*) to myosin distribution revealed in the same fixed cells (*b, d, f,* and *h*) by indirect immunofluorescence staining with myosin antibody and fluorescein-conjugated secondary antibody. Cells shown in (*e-h*) were treated with 500 nM of nocodazole for 20 h before myosin injection while cells in (*a-d*) were not treated. Cell regions shown in (*c, d,* and *g, h*) represent higher magnification views of the upper left edge of the cell shown in (*a* and *b*) and bottom right edge of the cell shown in (*e* and *f*), respectively. Both low and high magnification views show high degree of correlation between direct fluorescence in rhodamine channel and antibody staining detected in the same cell after fixation in fluorescein channel. In *b* and *f* regions of neighboring noninjected cells are seen. Nocodazole-treated and nontreated cells show similar myosin distribution patterns. Bars: (*a* and *e*) 10 μm; and (*c* and *g*) 2 μm.

tribution using both immunofluorescence staining (Weber and Groeschel-Stewart, 1974; Fujiwara and Pollard, 1976; Lawson, 1987) and direct imaging of injected myosin (McKenna et al., 1989) although the investigators usually tended to put more emphasis on the punctate or even periodic features of the myosin distribution.

To verify that microinjected xrho-myosin was colocalized with the endogenous cellular myosin, we performed indirect
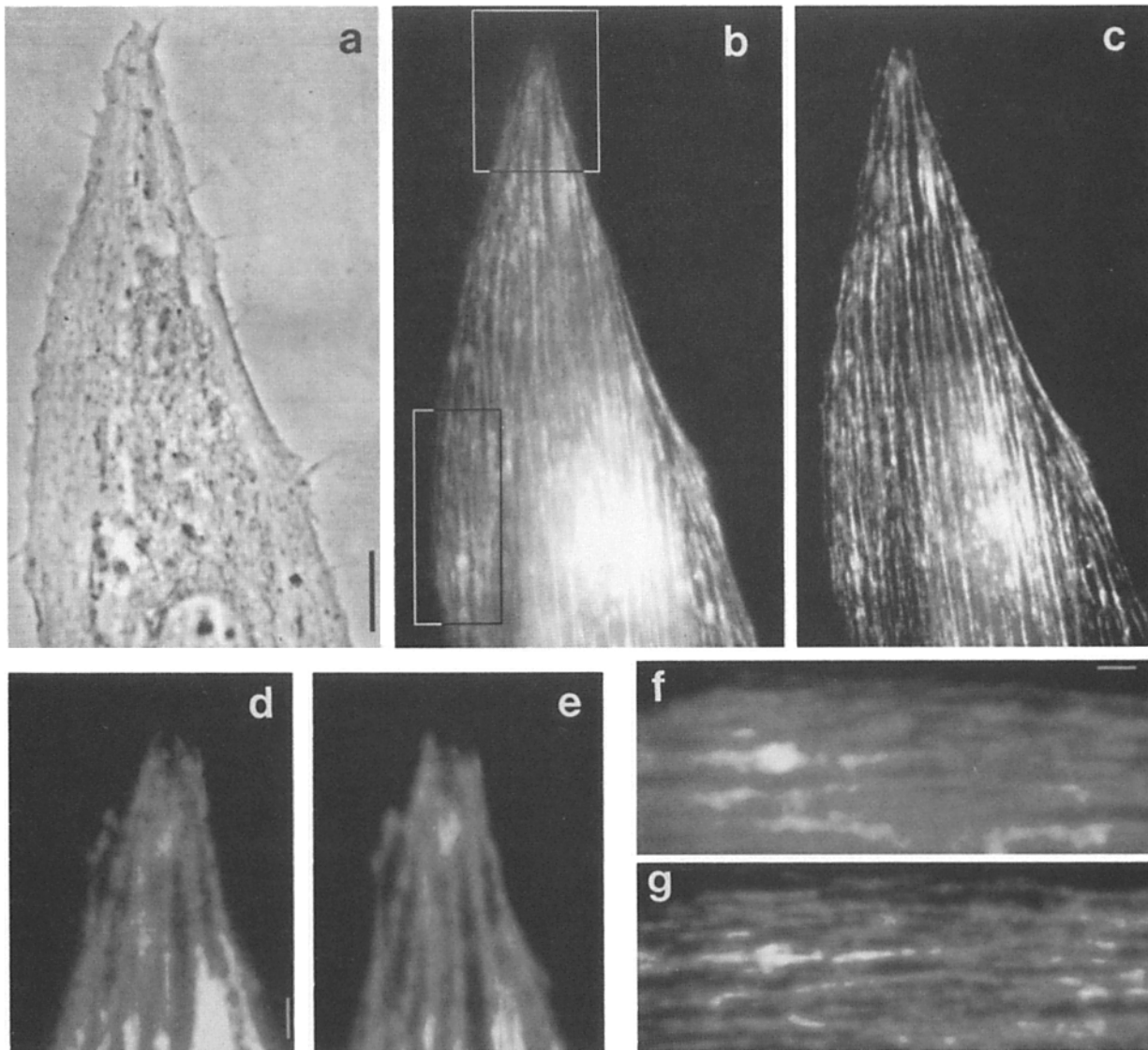
Figure 4. Absence of xrho-myosin redistribution upon extraction of nocodazole-treated fibroblast with Triton X-100 and treatment of cytoskeleton with gelsolin to remove actin. Phase micrograph (*a*) and xrho-myosin fluorescence (*b*) of a living cell; xrho-myosin fluorescence in the same cell after Triton X-100 extraction and gelsolin treatment (*c*). Enlarged fluorescent images of cell regions shown by boxes in *b*, in living cell (*d* and *f*) and after extraction and gelsolin treatment (*e* and *g*). Bars: (*a*) 10 μm; and (*d* and *f*) 2 μm.

immunofluorescence staining with myosin antibody on the same cells that were previously injected and observed in the living state. The very close concordance of direct fluorescence and immunofluorescence patterns was observed in both nocodazole-treated and nontreated cells (Fig. 3). The only difference was that living cells exhibited bright diffuse fluorescence in the central, thicker region apparently due to the presence of soluble myosin which was later removed upon extraction preceding antibody staining. Immunofluorescence staining also showed the broad variation in the relative abundance of continuous and punctate structures in injected as well as in neighboring noninjected cells.

Based on these results, we conclude that injected xrho-myosin incorporates into native myosin-containing structures resulting in both continuous and punctate fluorescence patterns. Nocodazole treatment did not significantly affect the mode of incorporation since similar continuous and punctate patterns were observed in untreated and nocodazole-treated cells.

Retention of Myosin Organization from Living Cells to EM Specimens

To evaluate the validity of the procedure used to display myosin ultrastructural organization it was necessary to compare myosin arrangement in living cells with its arrangement in the EM specimens. For the simplification of this analysis, we performed it in two steps. First, myosin distribution in living cells was compared to its distribution in actin-depleted cytoskeletons of the same cells by means of direct fluorescence microscopy. Second, myosin fluorescence patterns in actin-depleted cytoskeletons were compared to the arrangement of cytoskeletal structures seen in these same cytoskeletons by EM after dehydration, critical point drying and platinum and carbon coating.

Absence of Myosin Rearrangement upon Actin Extraction with Gelsolin. A major issue in direct fluorescence and immunofluorescence studies is whether redistribution and differential extraction of proteins occurs upon permeabilization of cultured cells (Melan and Sluder, 1992). Similar possibilities need also be considered for special conditions such as extraction of actin by gelsolin treatment. To determine whether detergent lysis and actin extraction from the cytoskeleton caused any redistribution of myosin, we compared patterns of myosin fluorescence in the living cell and in the same cell after Triton X-100 extraction and gelsolin treatment. Four separate cell extraction experiments were performed with one to four xrho-myosin–microinjected cells analyzed in each experiment (a total number of nine cells). A typical example is shown in Fig. 4 (*b* and *c*). As could be seen, myosin patterns in the living cell and actin-depleted cytoskeleton were almost identical. One difference was that in the extracted cell, unlike the living one, no diffuse fluorescence was observed. This can be explained by the absence of the soluble fraction of myosin in the extracted cell. The other change caused by extraction was that edges of myosin structures, especially in the central part of the cell, looked sharper in the image of the extracted cell than in the living state. This may be due to some flattening of the cytoskeleton during extraction which allowed for better focusing.

Close examination of selected areas of the cell at higher magnification (Fig. 4, *d* and *e*, *f* and *g*) revealed that every fluorescent fiber and spot in the living cell had its counterpart in the extracted cell; therefore, we concluded that no myosin structures were lost during extraction and their arrangement with respect to each other did not change significantly, at least as could be evaluated at the light microscopic level. A similar degree of retention of myosin distribution was observed in all lysed and gelsolin-treated cells.

Retention of Myosin Organization in Dried and Coated Specimens. Fig. 5 illustrates the correspondence of the fluorescence image of the gelsolin-treated cytoskeleton to the structural pattern revealed by EM of the replica of the same critical point dried cytoskeleton. It can be seen that while the fluorescent image represents a combination of separate spots and fibers with regions of weaker fluorescence between them, EM reveals a continuous network consisting of short filaments and their small bundles. Despite the apparent diversity of the two pictures, there was a close correlation between them: all fluorescent spots and fibers in Fig. 5 *a* corresponded in Fig. 5 *b* either to more dense areas in the filament network or to prominent filament bundles, whereas areas of lower fluorescence corresponded to sparse regions of the network. Vice versa, all the network densities or filament bundles in the electron microscopic image corresponded to fluorescent bright spots or patches. Single filaments visible in the electron microscopic image had no equivalent in the fluorescence picture, but such correlation obviously could not be expected because of the low-resolution limit of light microscopy. The other reason why small structures may not show up in the fluorescent image is that only a fraction of the myosin molecules present were fluorescently labeled, so small aggregates of myosin may statistically lack a labeled molecule and thus be nonfluorescent. However, all the groups of filaments correlated very well with the fluorescent spots and fibers. The only prominent features in the electron microscopic image that had no

counterpart in the fluorescent picture were aggregates of vesicle-like structures at the edge of the cytoskeleton. As will be shown more clearly in higher magnification images, these structures have the morphology of clathrin cages. Thus, the correspondence of the cytoskeleton pattern to the fluorescence image shows that preparation of the specimen for EM did not cause any significant change in myosin organization. In addition, the correlation of the distribution of the cytoskeletal structures to the myosin fluorescence further confirmed that all the other components of the cytoskeleton were indeed removed and what we looked at in the electron microscope was myosin. The close correlation of the density distribution of cytoskeletal network to the myosin fluorescence pattern was observed in all tested preparations, irrespective of whether the fluorescence distribution appeared punctate or continuous. The total number of cells that were correlatively examined in the light microscope and in the EM was limited because of the difficulties in recovering the same cell. However, we were able to successfully analyze a total of 16 cells in five independent gelsolin-treated preparations with 2 to 6 cells analyzed in each preparation.

Ultrastructural Analysis of Myosin Arrangement in Actin-depleted Cytoskeletons

To visualize the arrangement of myosin in the cytoskeletal network, we needed to examine specimens at higher magnification. Fig. 6 presents a higher magnification view of the two regions of the cell lamellum shown within boxes in Fig. 5. Major structural elements seen in these images were short filaments of variable thickness, having rather smooth rodlike central regions and thicker globular ends, shaped either as a single globular mass or several globular projections. These dumbbell-shaped filaments as analyzed from high-magnification micrographs (also see Fig. 8) had an average length of 330 nm (Fig. 7).

Schematic representation of the arrangement of these filaments, overlaid on the fluorescence myosin pattern of corresponding cellular regions is shown in Fig. 6 (*b* and *d*). Filaments were arranged in small bundles where individual filaments lay side by side (the center of Fig. 6 *a*), and in chains and networks, where individual filaments contacted each other at their terminal globular domains (Fig. 6 *c*). Filaments themselves, at least at their central rodlike regions were rather straight, but their aggregates often formed z-like structures, because at the sites of contact individual filaments were often oriented at sharp angles relative to each other.

Based on their characteristic morphology and on the similarity to the filaments previously identified in similar preparations by immunogold staining using myosin antibodies (Svitkina et al., 1989), we identified these short filaments as myosin bipolar filaments. In dense bundles, identification of myosin filaments was only putative, however in less dense regions of the lamellum they clearly accounted for most of the cytoskeletal mass. Besides myosin filaments, numerous clathrin cages, some amorphous vesicles and a few thin filaments of unknown nature were observed in the preparation. No identifiable actin filaments or microtubules were found in the specimen. In some regions of cell lamellae occasional intermediate filaments could be seen (not shown) but they were easily distinguishable from myosin filaments by their
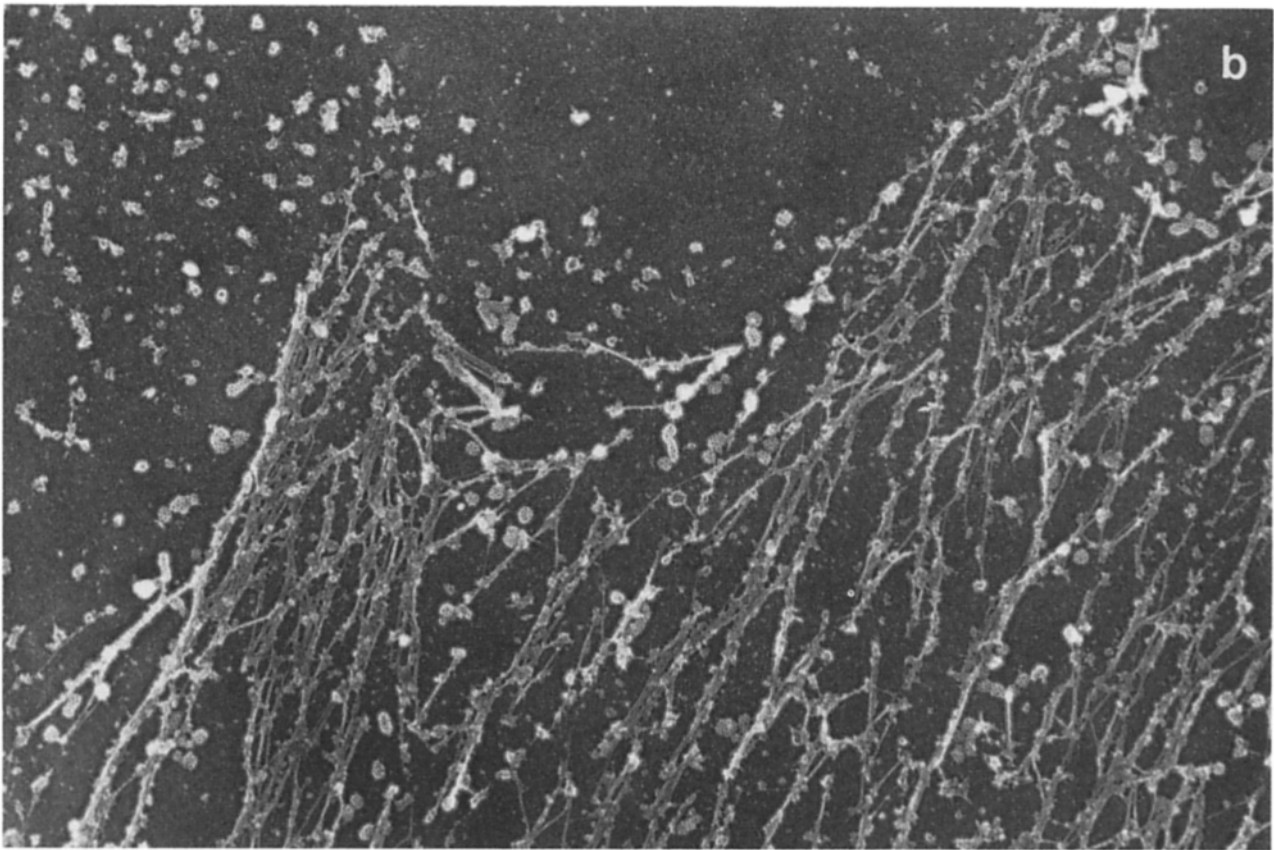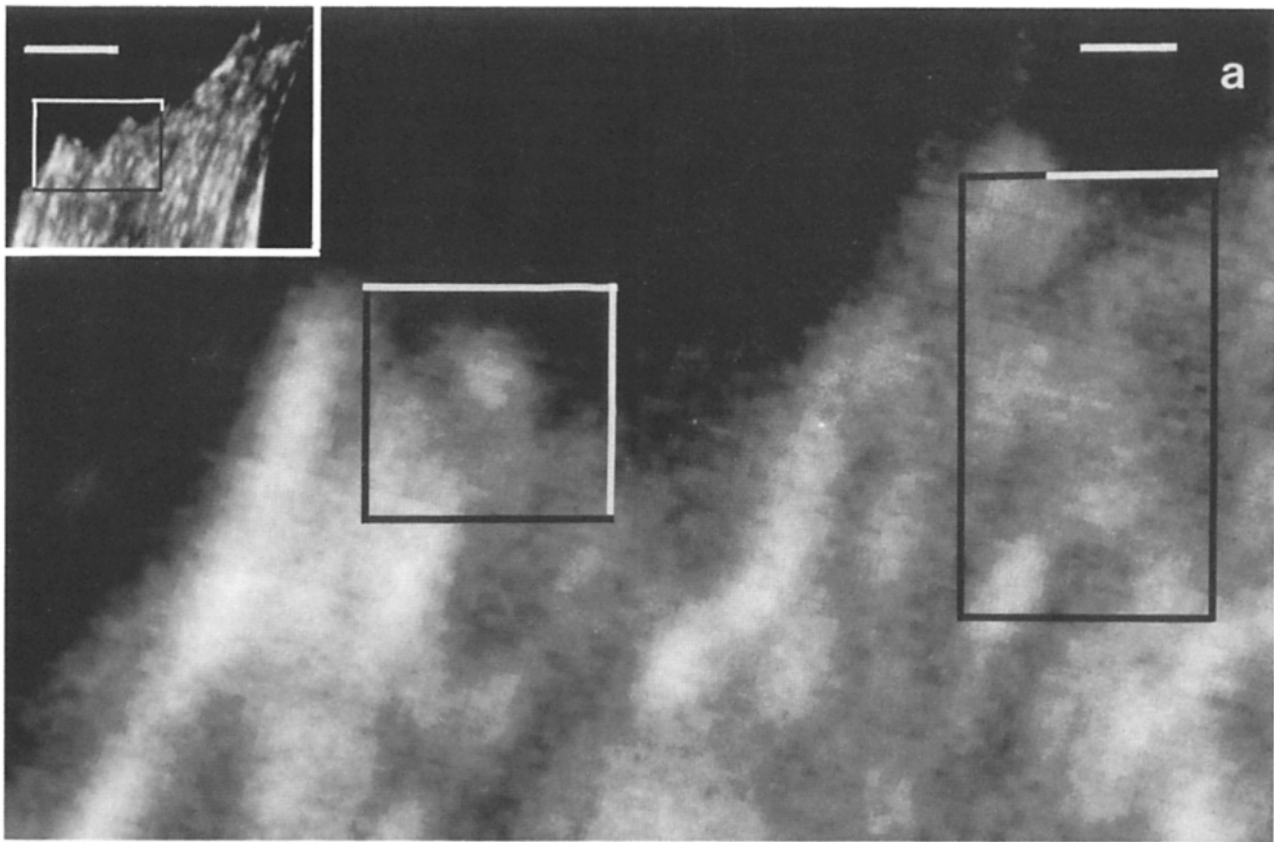
Figure 5. Correlation of myosin filament network revealed by EM of platinum replica (*b*) to the xrho-myosin distribution pattern in gelsolin-treated cytoskeleton (*a*). Inset in *a* shows lower magnification fluorescence view of the same cell. Boxed area of the cell lamellum in the inset corresponds to the region shown in the main picture. Bars: (*a*) 500 nm; (inset) 5 μm.

wavy morphology and frequent branching. Superimposition of the diagram of bipolar filament arrangement on fluorescent images of the corresponding regions of the lamellum allowed us to analyze the underlying ultrastructure of the features of the myosin fluorescence pattern. In Fig. 6 (a and b) two connected bundles consisting of several filaments each clearly correspond to a separate myosin fluorescence spot (Fig. 6 b, arrow). Interestingly, these bundles are connected to a dense filament mass by several filaments (Fig. 6 b, arrowheads) forming a structure reminiscent of an extendible holder, suggesting a possibility of an extension of these bundles relative to the rest of the filaments. Fig. 6 (c and d) shows that apparent punctate fluorescence at the light microscopic level does not necessarily indicate discrete structures at the electron microscopic level. The arrangement of several fluorescent spots with rather vague boundaries in fact corresponds to a continuous network of interconnected myosin filaments.

A similar end-to-end myosin filament arrangement was observed in all cytoskeletal preparations of microinjected and gelsolin-treated cells that exhibited sparse enough cytoskeletal network to make possible the identification of individual filaments. A similar arrangement was also observed in sparse regions of cytoskeletons of numerous neighboring noninjected cells in the same replica preparations as well as in replicas prepared separately from gelsolin-treated cytoskeletons of noninjected cells. In total, more than 50 cells in eight separate preparations were analyzed at the EM level.

To determine the range of conditions under which the described myosin arrangement is stable, we also analyzed cytoskeletal preparations extracted and treated with gelsolin in different buffer solutions (8 to 15 cells were analyzed by EM for each set of conditions). Bipolar myosin filaments of identical size and morphology as in our standard preparations were clearly seen when a higher pH and ionic strength buffer (modified PHEM buffer of Schliwa and van Blerkom, 1981—see Materials and Methods for details) was used for extraction and incubation with gelsolin. As in our standard conditions, most of the filaments contacted each other at their ends while being oriented relative to each other at a variety of angles. However, under these conditions the filament network was less dense and was generally continuous over a shorter distance (sometimes only over three to five lengths of individual filament). This probably indicated that higher pH and ionic strength buffer induced partial solubilization of myosin and fragmentation of the network during the long-term incubation with gelsolin. In agreement with this interpretation, immunofluorescence microscopy of these preparations also showed a less dense arrangement of myosin than in living cells, and cells extracted under our standard conditions. In particular, preparations in modified PHEM buffer were depleted of regions showing fine punctate or networklike myosin distribution, while discrete myosin-containing fibers were usually present although frequently bent and fragmented. Higher pH probably played a more important role in fragmentation of myosin network than higher ionic strength because the same results were obtained with modified PHEM buffer lacking or containing up to 100 mM KCl.

Addition of 1 mM ATP to modified PHEM buffer (either with 100 mM KCl or without it) resulted in complete solubilization of myosin during incubation with gelsolin as was shown by immunofluorescence microscopy. Extraction of myosin can be accounted for by a combination of two factors: ATP-induced increase in critical concentration for myosin polymerization; and dilution of depolymerized myosin by the extraction medium (see Discussion). In agreement with light microscopy, bipolar filaments were no longer seen in EM preparations. It should be noted that incubation with ATP without gelsolin, even at 4°C, also resulted in extraction of most of the myosin and in major distortion of the actin pattern (bending of fibers and formation of asterlike structures), so overall cytoskeletal organization was not conserved under this condition. Thus, a myosin filament network was observed under a variety of buffer conditions (except the presence of ATP) but our standard extraction buffer (modified after Avnur et al., 1983) was best for the preservation of a myosin distribution similar to the one in living cells.

Fig. 8 shows a gallery of different patterns of myosin arrangement in noninjected (a-e) as well as injected (f) cells treated under our standard conditions. Sometimes we observed individual myosin bipolar filaments (usually at the very edge of cytoskeleton) (Fig. 8, a and b). More often, individual filaments (Fig. 8 c) or filament bundles (Fig. 8 d) formed a network, in which polygons could be recognized as one of the common arrangements. Sometimes we saw long bundles of regularly arranged filaments (Fig. 8 e) similar to the bundles described earlier in cytoskeletons, sonicated after actin extraction (Svitkina et al., 1989). Finally, in Fig. 8 f, the myosin network in what seems to be a ruffling area of the cell is represented. In this region, the filament network seems to be compressed in a direction perpendicular to the cell edge with the groups of filaments forming z-like structures and orienting nearly parallel to the edge. In summary, the observed pattern of myosin arrangement could be described as a variable network constituted of bipolar filaments.

Discussion

Evaluation of the Procedure Used to Visualize Myosin Organization

The present work aimed to answer the question: what is the ultrastructural organization of myosin in the living fibroblast. To solve this problem we sought to visualize myosin at the ultrastructural level and do so under conditions that do not induce at the same time significant changes in its arrangement. In accord with an earlier report (Svitkina et al., 1989) we have found that myosin filaments could be visualized after depleting the cytoskeleton of major fibrillar structures: microtubules, intermediate filaments, and actin filaments. We needed to check whether this depletion technique perturbed the organization of myosin itself.

Microtubules were removed by depolymerization with nocodazole. To concentrate the intermediate filaments to the perinuclear region and make the cell periphery free of these structures, we used prolonged incubation of the living cells with nocodazole. Although nocodazole is a specific microtubule depolymerizing drug and has no documented direct effect on the actomyosin system, it induced partial cell depolarization and rounding that was associated with re-
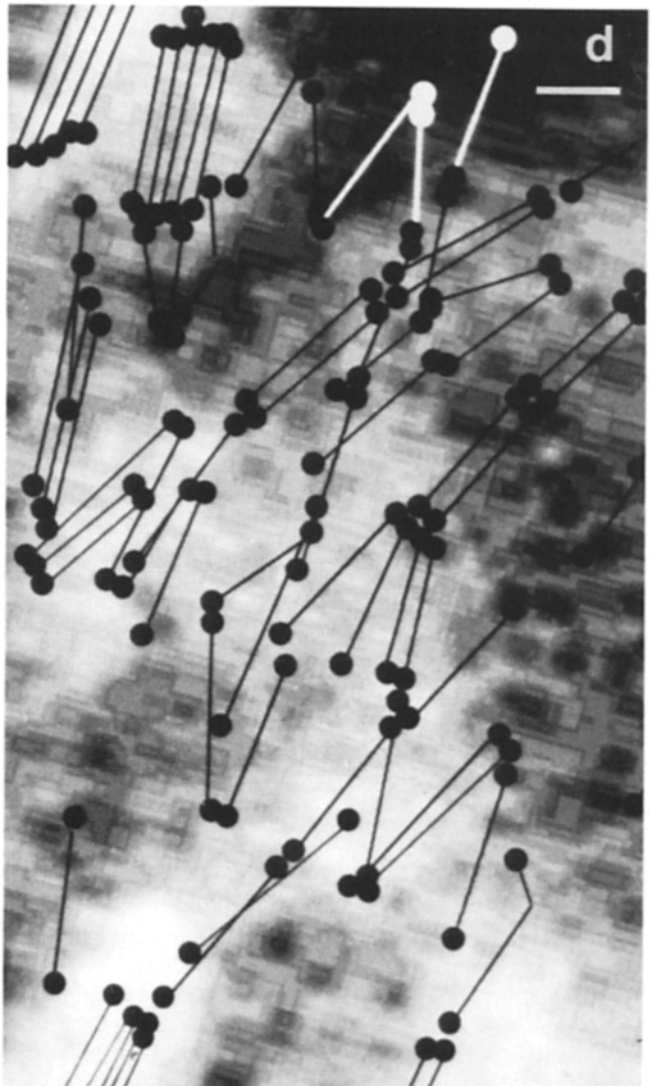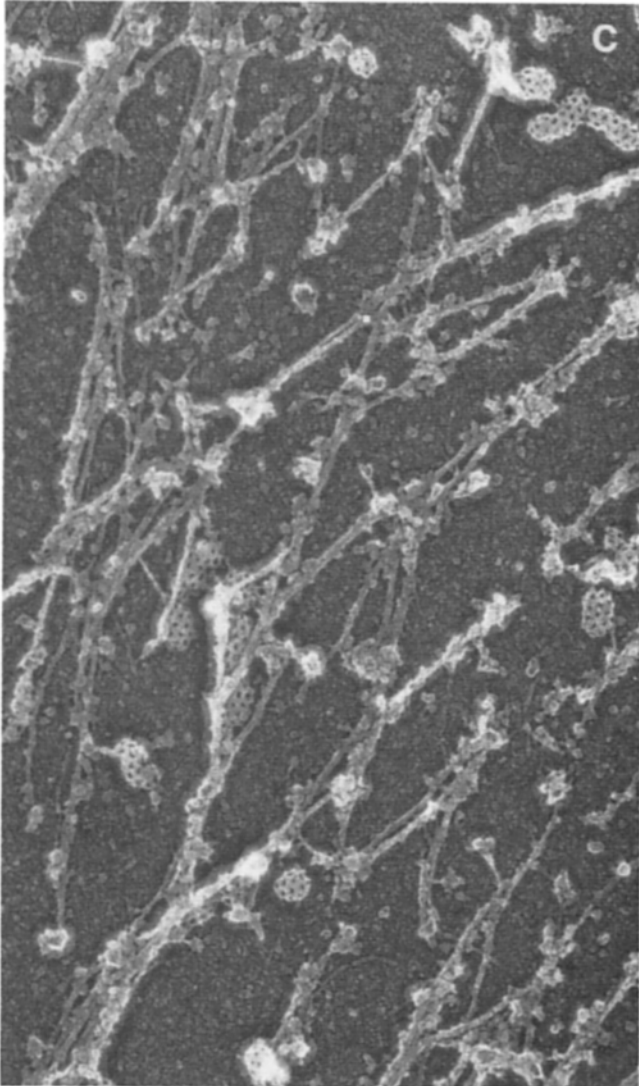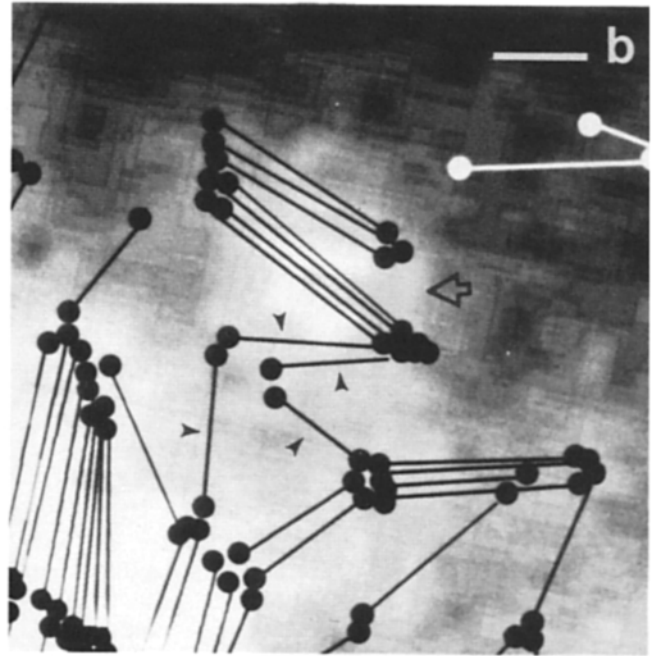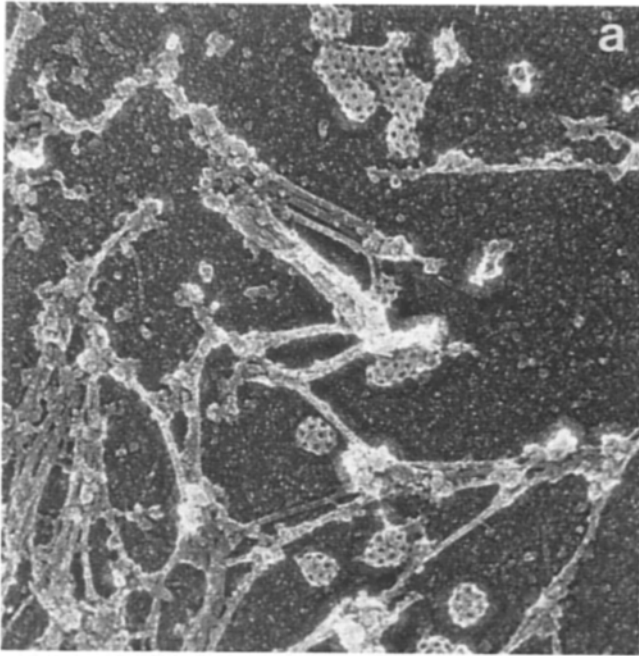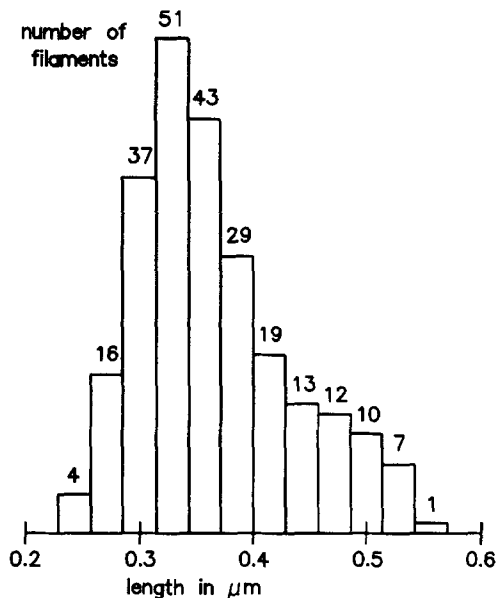
Figure 7. Length distribution of myosin filaments observed in platinum replica of fibroblast cytoskeleton.

configuration of all cell components, so some effect on the myosin II arrangement could not be excluded. To evaluate the effect of nocodazole treatment, comparison of myosin distribution in the same cell before and after treatment would not be informative because during the time of treatment significant myosin rearrangement should occur even in a cell not subjected to nocodazole due to the natural processes of cell locomotion and change in cell shape. However, when we observed whole populations of nocodazole treated and control cells by either direct fluorescence or immunofluorescence microscopy, we found no significant differences in myosin distribution patterns. Therefore, it seems likely that myosin II organization in nocodazole-treated cells is fundamentally the same as in the cells not subjected to pharmacological treatment.

The other steps of the procedure used to visualize myosin filaments were cell lysis in a slightly acidic buffer, a condition that stabilizes the myosin filaments (Reisler et al., 1986; Kuczmarski et al., 1987; Trybus and Lowey, 1987; Sinard and Pollard, 1989), treatment of the cytoskeletons with gelsolin to remove actin, chemical fixation, critical point drying, and platinum and carbon coating. The preservation of myosin structure through these steps was directly evaluated by comparison of myosin distribution in the same cell before and after the treatment. We found very good concordance between the xrho-myosin distribution in the living cell and its distribution in the actin-depleted cytoskeleton, and between the xrho-myosin fluorescence pattern in the actin-depleted preparation and the myosin filament network revealed by EM. These results demonstrated that the myosin

arrangement was not significantly altered during preparation.

We cannot exclude completely some local changes in myosin organization which were not detectable on the light microscopic level. However, significant ultrastructural rearrangement that resulted in no visible change in the overall myosin distribution pattern is not a likely possibility. In particular, if separated myosin filaments approached each other and formed a continuous network during the preparation procedure, it should result also in an overall shrinking of the cytoskeleton or in numerous local aggregations with gaps forming between aggregation sites. These effects should be detectable by light microscopy but neither of them was in fact observed when we compared the myosin distribution in living cells to the one after extraction and depletion of actin under our standard conditions. Observation of a similar myosin arrangement after extraction of the cells under different conditions also argues against the possibility that the myosin network could result from aggregation in the extraction media. As evaluated by light microscopy, higher pH and ionic strength media did not preserve the overall myosin distribution. Yet, under these conditions, pockets of myosin network were still detectable in the EM, suggesting that assemblies of bipolar filaments are fundamental building blocks in myosin organization.

Myosin networks were not detected when ATP was included in the extraction medium, under which condition myosin was removed from the cytoskeleton as documented by immunofluorescence microscopy. This extraction is consistent with the results of in vitro studies showing that the critical concentration for polymerization of dephosphorylated and, to a lesser extent, phosphorylated myosin increases in the presence of ATP (Suzuki et al., 1978; Cross et al., 1986; Kendrick-Jones et al., 1987). In the intact cell, although myosin is in the presence of ATP, substantial amounts of polymer are present, presumably because total myosin levels are above the critical concentration for assembly (0.5 mg/ml for dephosphorylated brush border myosin) (Kendrick-Jones et al., 1987). Upon permeabilization, all cytoplasmic molecules, including myosin are diluted by the large volume of the extraction buffer. Therefore, continued incubation in an ATP-containing medium would be expected to lead to complete solubilization of myosin. Similar properties have been reported for smooth muscle, dephosphorylated myosin, which is present in the form of filaments in situ (Somlyo et al., 1981) but is completely solubilized by ATP in vitro (Suzuki et al., 1978; Cross et al., 1986).

Another consideration is whether the myosin networks resulted from superposition of several layers of cytoskeletal structures. We think this is unlikely because lamellar regions of the cytoskeleton were very well spread and essentially one layered at the light microscopic level. When we examined these regions in living cells by direct fluorescence microscopy we noticed that only one set of myosin-containing

Figure 6. Myosin filament arrangement in the fibroblast cytoskeleton. Platinum replicas of regions of the cytoskeleton shown by boxes in Fig. 5 *a*, diagrams of myosin filament arrangement superimposed on the xrho-myosin distribution patterns in the same regions (*b* and *d*). Myosin filaments are represented as black stick and ball figures (each ball corresponds to the cluster of myosin heads at the end of the filament and stick symbolizes rodlike central region of the filament) on light regions and as white figures on dark regions. Bars, 200 nm.

648
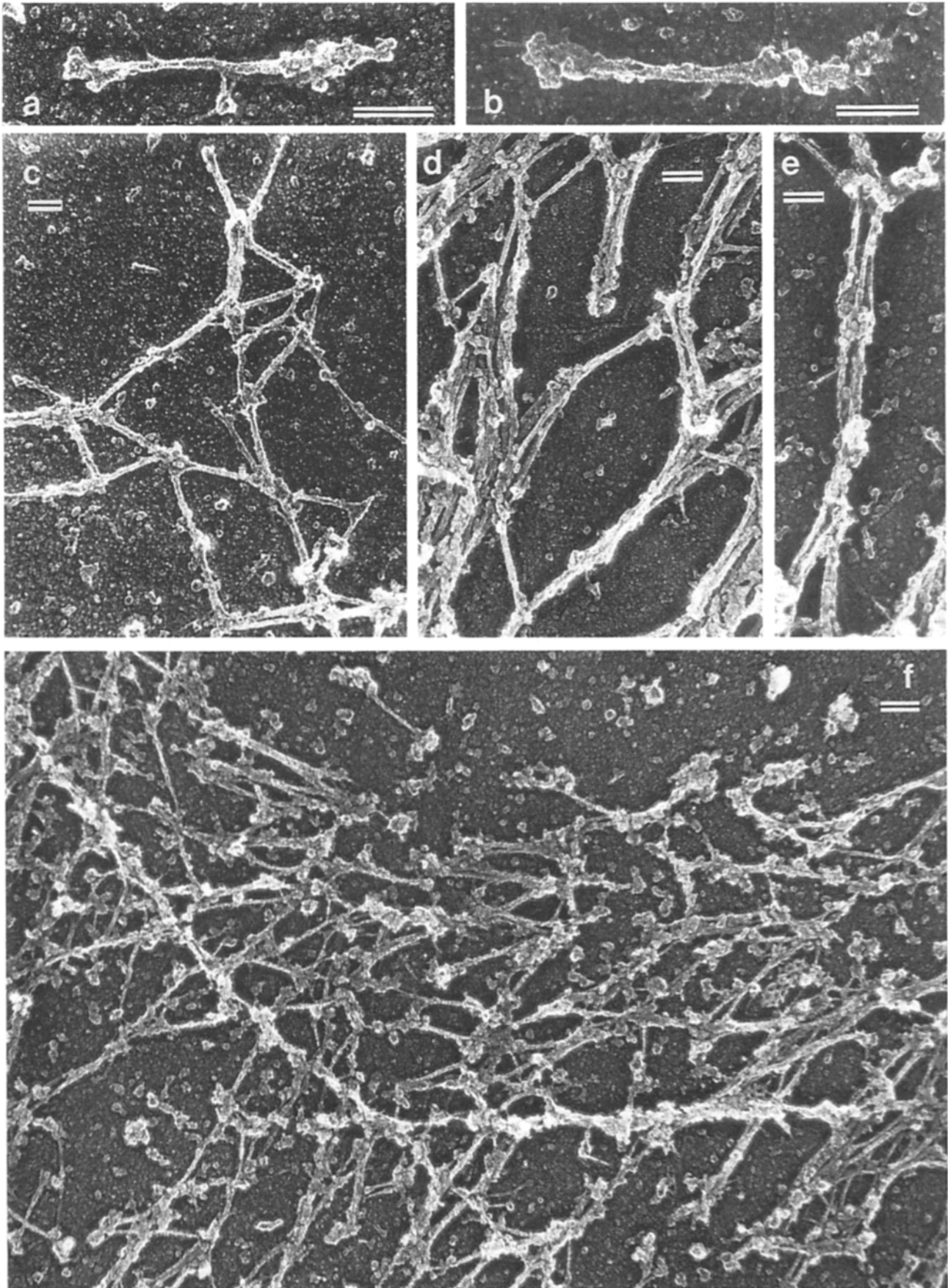
structures could be detected independently of the focus position. Changing the focal plane resulted in blurring of the image, but never in the observation of another set of fluorescent spots or fibers. In contrast, in regions closer to the nucleus which we did not analyze in detail here, multi-layered structures were clearly detectable both by fluorescence and electron microscopy. Based on the estimation of the depth of field for optical microscope (500 nm for red light and an oil-immersion lens with numerical aperture of 1.3) (see Inoué, 1986, page 118), we conclude that all the myosin structures in the lamellum were contained in a layer less than or equal to 500-nm thick.

The third issue to consider is whether the observed cytoskeletal network was induced by injection of exogenous myosin. Several lines of evidence argue against this possibility. First, injected myosin was localized by fluorescence microscopy in the same structures as endogenous cell myosin. Second, similarly looking networks of myosin bipolar filaments were also observed in noninjected cells both in the present work (Fig. 7, c–e) and in an earlier report (Svitkina et al., 1989). Finally, the amount of the injected myosin did not exceed 25% of the endogenous cell myosin (assuming the injected and endogenous myosin concentrations 5 and 1 mg/ml, respectively, and injected volume 5% of the cell volume). Simple calculation, in fact, shows that there is enough endogenous myosin in the cell to build a continuous cytoskeletal network. Assuming the concentration of myosin is 1 mg/ml (Niederman and Pollard, 1975), all the myosin is filamentous, and the average filament consists of 20 molecules, then a cell lamellum 0.3-μm thick will contain approximately 20 myosin filaments per square micrometer. Assuming that the length of the filament is 0.33 μm, 18 filaments per square micrometer would be enough to build a two-dimensional square network with the unit size equal to the length of the filament. If gaps are introduced in the network, then the number of filaments required is correspondingly reduced.

We conclude that the observed myosin arrangement in the form of extended networks of short bipolar filaments most probably reflects the actual myosin ultrastructural organization in the living cell.

Myosin Filaments in the Cytoskeleton

The visualization of short bipolar filaments is consistent with results of in vitro studies demonstrating that nonmuscle myosin II readily forms filaments under physiological salt conditions (Kendrick-Jones et al., 1987; Sinard and Pollard, 1990; for review see Korn and Hammer, 1988; Trybus, 1991). The assembly of mammalian cytoplasmic myosin II is stimulated by light chain phosphorylation. However, dephosphorylated myosin is also able to form filaments, although with higher critical concentration (Kendrick-Jones et al., 1987). Since a considerable portion of cytoplasmic myosin is normally phosphorylated in the cell (Lamb et al., 1988; Fernandez et al., 1990), it seems reasonable that a major part of the myosin in nonmuscle cells should be filamentous. Failure to identify myosin filaments in the cytoskeleton by standard

electron microscopy was probably due as discussed earlier (Niederman and Pollard, 1975; Svitkina et al., 1989) to the similarity of the diameter of the central rod-like portion of myosin filaments to the diameter of actin and intermediate filaments. Unlike Dictyostelium amoeboid cells where myosin II filaments were found primarily at the uroide region (Fukui et al., 1989), myosin II in fibroblasts is distributed throughout the cytoplasm except for the very leading edge (Zigmond et al., 1979; Conrad et al., 1989). Accordingly, we found myosin II filaments in the peripheral well-spread regions of the cells. Central regions contained very dense cytoskeletal structures which did not allow for clear morphological identification of individual filaments.

Myosin filaments that we observed in the cytoskeleton were similar in size to the filaments formed in vitro by many nonmuscle myosins (Niederman and Pollard, 1975; Burridge and Bray, 1975; Citi et al., 1987; Kuczmarski et al., 1987), and to minifilaments of striated and smooth muscle myosin (Reisler et al., 1980; Trybus and Lowey, 1985), but were slightly larger than octameric minifilaments of Acanthamoeba myosin II (Sinard et al., 1989). Striated and smooth muscle myosin minifilaments contain 16 to 18 (Reisler et al., 1980) and 12 to 14 myosin molecules (Trybus and Lowey, 1987), respectively, and filaments of platelet myosin were reported to contain 28 molecules (Niederman and Pollard, 1975). The resolution of our EM images was not sufficient to determine the number of myosin molecules in the filaments but, based on filament size, we estimate this number to be in the range of 10 to 30 molecules. Considerable variation in the length and diameter of the filaments and the detailed morphology of their termini indicated that probably there was variation in the number of molecules per filament. We did not identify side polar (Trybus and Lowey, 1987) or long bipolar filaments in our preparations. However, these forms of myosin might be present in the dense aggregates where individual filaments were not clearly distinguishable.

Myosin Filament Network—a New Type of Cytoskeletal Structure

The fairly continuous character of the myosin filament network, even in regions of apparently punctate fluorescence, suggests that myosin forms a cytoskeletal system of its own. This may explain our seemingly remarkable observation that the myosin distribution did not change significantly upon depletion of actin. The important questions raised by our findings are: (a) what is the nature of the links holding myosin filaments together; and (b) what is the functional significance of the myosin network.

Interfilament bonds may be formed either as a result of direct interaction between myosin heads themselves, or their indirect linkage via some associated protein(s). The formation of aggregates similar to those described in this paper was reported in preparations of purified nonmuscle myosin (Burridge and Bray, 1975; Hesketh et al., 1978) and in preparations of muscle myosin minifilaments (Podlubnaya et al., 1987) in vitro. On the other hand, I-protein from muscle was

---

Figure 8. Examples of myosin filament structures in fibroblast cytoskeleton: single filaments (a and b), filament networks (c and d), filament bundles (e), and filament arrangement in ruffling region of the cell (f). Images (a–e) were taken from the cytoskeletons of cells not injected with exogenous myosin and image (f) represents a region of an injected cell cytoskeleton. Bars, 100 nm.

reported to stimulate formation of cagelike aggregates of muscle myosin filaments (Ohashi et al., 1989). Similar protein(s) may be involved in filament aggregation in fibroblasts.

Regarding the functional significance of the myosin network, one can speculate that it plays a role in maintaining cell shape and organizing other cytoskeletal components. Of different types of nonmuscle myosin molecules, filament-forming myosin II is a likely candidate to contribute to the structural organization of the cell (see Herman et al., 1981), whereas non-polymerizable myosin I may function primarily as a molecular translocator. Indeed, experiments using myosin II inactivation were suggestive of its structural cytoskeletal function (see Introduction for references).

Although a continuous network of myosin filaments provides a natural explanation for its structural cytoskeletal role, it is not immediately obvious whether this mode of organization is also consistent with the well-established role of myosin II in cell contractility. Contraction in living or permeabilized cultured cells was reported to be associated with the reduction of the distance between myosin (Giuliano and Taylor, 1990) or α-actinin (Kreis and Birchmeier, 1980) containing spots. This seems to be in favor of a sarcomeric contraction mechanism which requires that initially distant arrays of myosin filaments approach each other. However, studies of myosin dynamics in living cells (McKenna et al., 1989; Giuliano and Taylor, 1990) indicated that myosin behavior is complex and there are different types of myosin rearrangement besides shortening of the sarcomeric units.

A sarcomeric type of myosin organization may exist in well-developed stress fibers. However, in the cell lamellum, we observed a continuous filament network rather than a sarcomeric structure. This network may represent one of the possible modes of myosin dynamic organization and be interconvertable with the sarcomeric mode. We asked what type of structural rearrangement could be based on the geometry of the myosin network and how it could be involved in cell contractility.

Hypothesis on Myosin Network Reorganization Mechanism

The remarkable feature of the myosin filament network is the variability of angles at which contacting bipolar filaments are oriented with respect to each other (see Figs. 6 a, and 8, c and f). This variability may reflect variability of orientation of actin filaments with which myosin filaments are probably interacting. An alternative explanation is that the variability of myosin orientation reflects the different stages in the dynamic reorganization of the myosin network.

A hypothetical mechanism for such reorganization is illustrated in Fig. 9. This mechanism uses the same filament sliding principle on which the mechanism of striated muscle contraction is based (Huxley, 1973), but introduces a new actomyosin geometry, differing from the classical scheme in two features: (a) myosin filaments are bound to each other in the network where they have freedom to rotate around sites of their contact; and (b) actin filaments are not parallel to myosin filaments throughout the "contraction" event.

As a starting condition, we consider a configuration that may exist in a region behind the leading edge of the cell or in an established cell protrusion (Conrad et al., 1989) which is about to retract. We assume that an array of actin filaments, partially aligned parallel to each other and to the edge
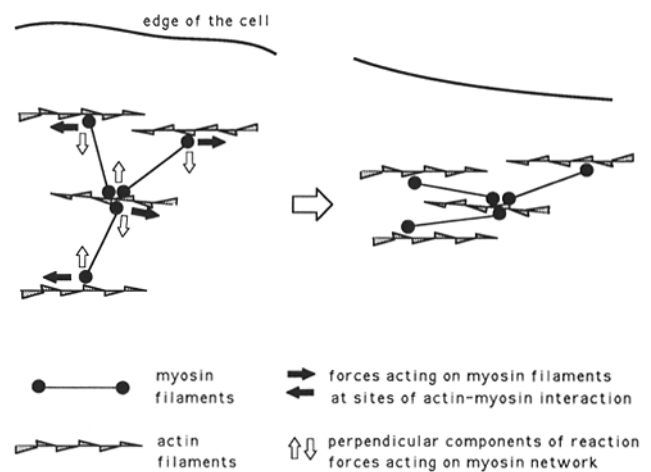

Figure 9. Diagram illustrating the hypothesis of the mechanism of myosin filament network rearrangement. Randomly oriented bipolar myosin filaments that are bound to each other in a network slide along actin filaments aligned parallel to the edge of the cell. Perpendicular components of reaction forces acting on the myosin network cause the bipolar filaments to rotate about sites of head-to-head contact. As a result, the myosin network stretches parallel to the cell edge and condenses in the perpendicular direction.

of the cell (Heath, 1983) but having no preferential polarity (Begg et al., 1978; Sanger and Sanger, 1980; Lewis and Bridgman, 1992) interacts with a network of randomly oriented interconnecting myosin filaments. A random initial orientation of myosin filaments is reasonable to assume if myosin recently appeared in the peripheral region of the cell and was assembled into a network. Because of the flexibility of the myosin head (Reedy et al., 1989; Toyoshima et al., 1989), myosin filaments will be able to interact with actin and move sideways in the direction dictated by actin filament polarity (Fig. 9, *filled arrows*), even if myosin and actin filaments are not aligned. Because myosin heads maintain contact with other myosin filaments in the network, the filaments will be restricted in their sideways motion. Some of the filaments in the network will interact with actin filaments of opposite polarity and exert forces of opposite direction on the other filaments in the network. This will lead to rotation of filaments around their sites of contact as flexible joints and to the overall change of network configuration.

In general, forces generated at sites of interaction with actin will be transmitted throughout the network. This means that forces exerted parallel to the long axis of actin filaments will induce reactive force components causing displacements of myosin filaments in a perpendicular direction. Eventually, independent of the precise initial configuration, the network will be stretched along actin filaments and "contracted" in the perpendicular direction. Net tension will be developed not only along actin filaments, as implicated by the classic sarcomeric mechanism, but also perpendicular to the orientation of actin, that is, in radial direction in the case of actin filaments parallel to the cell edge. Therefore, actin filament bundles oriented perpendicular to the direction of cell locomotion which are usually observed behind the leading edge of the cell may not only function in lateral stabilization of a locomoting cell as was proposed (Conrad et al., 1989) but also be involved in generation of tension along the

axis of cell locomotion pulling the cell body after the leading edge.

References

Adams, R. J., and T. D. Pollard. 1989. Membrane-bound myosin I provides new mechanisms in cell motility. *Cell Motil. Cytoskeleton.* 14:178-182.

Avnur, Z., J. V. Small, and B. Geiger. 1983. Actin-independent association of vinculin with the cytoplasmic aspects of plasma membrane in cell contact areas. *J. Cell Biol.* 96:1622-1630.

Begg, D. A., R. Rodewald, and L. I. Rebhun. 1978. The visualization of actin filament polarity in thin sections: evidence for the uniform polarity of membrane associated filaments. *J. Cell Biol.* 79:846-852.

Bershadsky, A. D., and J. M. Vasiliev. 1988. Cytoskeleton. Plenum Press, New York. 218-222.

Burridge, K., and D. Bray. 1975. Purification and structural analysis of myosins from brain and other non-muscle tissues. *J. Mol. Biol.* 99:1-14.

Byers, H. R., G. E. White, and K. Fujiwara. 1984. Organization and function of stress fibers in cells in vitro and in situ. *In* Cell and Muscle Motility. Vol. 5. J. W. Shay, editor. Plenum Publishing Corp. 83-137.

Cheney, R. E., and M. S. Mooseker. 1992. Unconventional myosins. *Curr. Opin. Cell Biol.* 4:27-35.

Citi, S., R. C. Smith, and J. Kendrick-Jones. 1987. Effect of light chain phosphorylation and skeletal myosin on the stability of non-muscle myosin filaments. *J. Mol. Biol.* 198:253-262.

Clarke, M., and J. A. Spudich. 1977. Nonmuscle contractile proteins: the role of actin and myosin in cell motility and shape determination. *Annu. Rev. Biochem.* 46:797-822.

Conrad, P. A., M. A. Nederlof, I. M. Herman, and D. L. Taylor. 1989. Correlated distribution of actin, myosin and microtubules at the leading edge of migrating Swiss 3T3 fibroblasts. *Cell Motil. Cytoskeleton.* 14:527-543.

Cross, R. A., K. E. Cross, and A. Sobieszek. 1986. ATP-linked monomer-polymer equilibrium of smooth muscle myosin: the free folded monomer traps ADP.P_i. *EMBO (Eur. Mol. Biol. Organ.) J.* 5:2637-2641.

De Brabander, M., R. Van de Veire, R. Aerts, M. Borgers, and P. Janssen. 1976. The effects of methyl[5-(2-Thienylcarbonyl)-1H-benzimidazol-2-yl]carbamate (R 17 934, NSC 238159), a new synthetic antitumoral drug interfering with microtubules, on mammalian cells cultured in vitro. *Cancer Res.* 36:905-916.

De Brabander, M., G. Geuens, R. Nuydens, R. Willebrords, and J. De Mey. 1982. Microtubules stability and assembly in living cells: the influence of metabolic inhibitors, taxol and pH. *Cold Spring Harbor Symp. Quant. Biol.* 46:227-240.

De Lozanne, A., and J. A. Spudich. 1987. Disruption of the *Dictyostelium* myosin heavy chain gene by homologous recombination. *Science (Wash. DC).* 236:1086-1091.

Fernandez, A., D. L. Brautigan, M. Mumby, and N. J. C. Lamb. 1990. Protein phosphatase type-1, not type-2A, modulates actin microfilament integrity and myosin light chain phosphorylation in living nonmuscle cells. *J. Cell Biol.* 111:103-112.

Fleischer, M., and K. E. Wohlfarth-Bottermann. 1975. Correlation between tension force generation, fibrillogenesis and ultrastructure of cytoplasmic actomyosin during isometric and isotonic contractions of protoplasmic strands. *Cytobiologie.* 10:339-365.

Fujiwara, K., and T. D. Pollard. 1976. Fluorescence antibody localization of myosin in the cytoplasm, cleavage furrow, and mitotic spindle of human cells. *J. Cell Biol.* 71:848-875.

Fukui, Y., T. J. Lynch, H. Brzeska, and E. D. Korn. 1989. Myosin I is located at the leading edges of locomoting *Dictyostelium* amoebae. *Nature (Lond.).* 341:328-331.

Fukui, Y., A. De Lozanne, and J. A. Spudich. 1990. Structure and function of the cytoskeleton of a *Dictyostelium* myosin-defective mutant. *J. Cell Biol.* 110:367-378.

Geuens, G., M. De Brabander, R. Nuydens, and J. De Mey. 1983. The interaction between microtubules and intermediate filaments in cultured cells treated with taxol and nocodazole. *Cell Biol. Int. Reports.* 7:35-47.

Giuliano, K. A., and D. L. Taylor. 1990. Formation, transport, contraction and disassembly of stress fibers in fibroblasts. *Cell Motil. Cytoskeleton.* 16:14-21.

Goldman, R. D., and D. M. Knipe. 1972. Functions of cytoplasmic fibers in nonmuscle cell motility. *Cold Spring Harbor Simp. Quant. Biol.* 37:523-534.

Goldman, R. D., E. Lazarides, R. Pollack, and K. Weber. 1975. The distribution of actin in non-muscle cells. The use of actin antibody in the localization of actin within the microfilament bundles of mouse 3T3 cells. *Exp. Cell Res.* 90:333-344.

Gordon, W. E. 1978. Immunofluorescent and ultrastructural studies of "sarcomeric" units in stress fibers of cultured non-muscle cells. *Exp. Cell Res.* 117:253-260.

Heath, J. P. 1983. Behavior and structure of the leading lamella in moving fibroblasts. I. Occurrence and centripetal movement of arc-shaped microfilament bundles beneath the dorsal cell surface. *J. Cell Sci.* 60:331-354.

Herman, I. M., N. Crisona, and T. D. Pollard. 1981. Relation between cell activity and the distribution of cytoplasmic actin and myosin. *J. Cell Biol.* 90:84-91.

Hesketh, G. E., D. Aunis, P. Mandel, and G. Devilliers. 1978. Biochemical and morphological studies of bovine adrenal medullary myosin. *Biol. Cell.* 33:199-205.

Honer, B., S. Citi, J. Kendrick-Jones, and B. Jockusch. 1988. Modulation of cellular morphology and locomotory activity by antibodies against myosin. *J. Cell Biol.* 107:2181-2189.

Huxley, H. E. 1973. Muscular contraction and cell motility. *Nature (Lond.).* 243:445-449.

Ikebe, M., and D. Hartshorne. 1985. Effects of Ca^{2+} on the conformation and enzymatic activity of smooth muscle myosin. *J. Biol. Chem.* 260:13146-13153.

Inoué, S. 1986. Video Microscopy. Plenum Press, N. Y. and London. 118.

Kendrick-Jones, J., R. C. Smith, R. Craig, and S. Citi. 1987. Polymerization of vertebrate non-muscle and smooth muscle myosins. *J. Mol. Biol.* 198:241-252.

Knecht, D. A., and W. F. Loomis. 1987. Antisense RNA inactivation of myosin heavy chain gene expression in *Dictyostelium discoideum*. *Science (Wash. DC).* 236:1081-1086.

Knecht, D. A., and W. F. Loomis. 1988. Developmental consequences of the lack of myosin heavy chain in *Dictyostelium discoideum*. *Dev. Biol.* 128:178-184.

Korn, E. D., and J. A. Hammer, III. 1988. Myosins of nonmuscle cells. *Annu. Rev. Biophys. Biophys. Chem.* 17:23-45.

Kreis, T., and W. Birchmeier. 1980. Stress fiber sarcomeres of fibroblasts are contractile. *Cell.* 22:555-561.

Kuczmarski, E. R., S. R. Tafuri, and L. M. Parysek. 1987. Effect of heavy chain phosphorylation on the polymerization and structure of *Dictyostelium* myosin filaments. *J. Cell Biol.* 105:2989-2997.

Kwiatkowski, D. J., P. A. Jamney, and H. L. Yin. 1989. Identification of critical functional and regulatory domains in gelsolin. *J. Cell Biol.* 108:1717-1726.

Laemmli, U. K. 1970. Cleavage of structural proteins during the assembly of the head of bacteriophage T4. *Nature (Lond.).* 227:680-685.

Lamb, N. J. C., A. Fernandez, M. A. Conti, R. Adelstein, D. B. Glass, W. J. Welch, and J. R. Feramisco. 1988. Regulation of actin microfilament integrity in living nonmuscle cells by the cAMP-dependent protein kinase and the myosin light chain kinase. *J. Cell Biol.* 106:1955-1971.

Langanger, G., M. Moeremans, G. Daneels, A. Sobieszek, M. De Brabander, and J. De Mey. 1986. The molecular organization of myosin in stress fibers of cultured cells. *J. Cell Biol.* 102:200-209.

Lawson, D. 1987. Distribution of myosin and relationship to actin organization in cortical and subcortical areas of antibody-labelled, quick-frozen, deep-etched fibroblast cytoskeletons. *Cell Motil. Cytoskeleton.* 7:368-380.

Lazarides, E. 1975. Tropomyosin antibody: the specific localization of tropomyosin in nonmuscle cells. *J. Cell Biol.* 65:549-561.

Lazarides, E., and K. Burridge. 1975. alpha-actinin: immunofluorescent localization of a muscle structural protein in nonmuscle cells. *Cell.* 6:289-298.

Lewis, A. K., and P. C. Bridgman. 1992. Nerve growth cone lamellipodia contain two populations of actin filaments that differ in organization and polarity. *J. Cell Biol.* 119:1219-1244.

Mabuchi, I., and M. Okuno. 1977. The effect of myosin antibody on the division of starfish blastomeres. *J. Cell Biol.* 74:251-263.

Mabuchi, I., S. Tsukita, S. Tsukita, and T. Sawai. 1988. Cleavage furrow isolated from newt eggs: contraction, organization of actin filaments, and protein components of the furrow. *Proc. Natl. Acad. Sci. USA.* 85:5966-5970.

McKenna, N. M., Y.-L. Wang, and M. E. Konkel. 1989. Formation and movement of myosin-containing structures in living fibroblasts. *J. Cell Biol.* 109:1163-1172.

Melan, M. A., and G. Sluder. 1992. Redistribution and differential extraction of soluble proteins in permeabilized cultured cells. *J. Cell Sci.* 101:731-743.

Mittal, B., J. M. Sanger, and J. W. Sanger. 1989. Visualization of intermediate filaments in living cells using fluorescently labeled desmin. *Cell Motil. Cytoskeleton.* 12:127-138.

Niederman, R., and T. D. Pollard. 1975. Human platelet myosin. II. In vitro assembly of myosin and structure of myosin filaments. *J. Cell Biol.* 67: 72-92.

Ohashi, K., K. Ishikawa, and K. Maruyama. 1989. I-Protein forms cage-like aggregates of myosin in vitro. *J. Biochem.* 106:104-109.

Pasternak, C., J. A. Spudich, and E. L. Elson. 1989. Capping surface receptors and concomitant cortical tension are generated by conventional myosin. *Nature (Lond.).* 341:549-551.

Podlubnaya, Z. A., D. I. Levitsky, L. A. Shuvalova, and B. F. Poglazov. 1987. Ordered assemblies of myosin minifilaments. *J. Mol. Biol.* 195:729-739.

Pollard, T. D., S. K. Doberstein, and H. G. Zot. 1991. Myosin-I. *Annu. Rev. Physiol.* 53:653-681.

Pruss, R. M., R. Mirsky, M. C. Raff, R. Thorpe, A. J. Dowding, and B. H. Anderton. 1981. All classes of intermediate filaments share a common antigenic determinant defined by a monoclonal antibody. *Cell.* 27:419-428.

Reedy, M. C., C. Beall, and E. Fyrberg. 1989. Formation of reverse rigor chevrons by myosin heads. *Nature (Lond.).* 339:481-483.

Reisler, E., P. Cheng, N. Borochov, and J. A. Lake. 1986. Monomers, dimers and minifilaments of vertebrate skeletal myosin in the presence of sodium pyrophosphate. *Biochemistry.* 25:326-332.

Reisler, E., S. Craig, and S. George. 1980. Myosin minifilaments. *J. Mol. Biol.* 143:129-145.

Ris, H. 1985. The cytoplasmic filament system in critical point-dried whole mounts and plastic-embedded sections. *J. Cell Biol.* 100:1474-1487.

Sanger, J. M., and J. W. Sanger. 1980. Banding and polarity of actin filaments in interphase and cleaving cells. *J. Cell Biol.* 86:568-575.

Schliwa, M., and J. van Blerkom. 1981. Structural interaction of cytoskeletal components. *J. Cell Biol.* 90:222-235.

Sinard, J. H., and T. D. Pollard. 1989. The effect of heavy chain phosphorylation and solution conditions on the assembly of *Acanthamoeba myosin II. J. Cell Biol.* 109:1529-1535.

Sinard, J. H., and T. D. Pollard. 1990. *Acanthamoeba* myosin II minifilaments assemble on a millisecond time scale with rate constants greater than those expected for a diffusion limited reaction. *J. Biol. Chem.* 265:3654-3660.

Sinard, J. H., W. F. Stafford, and T. D. Pollard. 1989. The mechanism of assembly of *Acanthamoeba* Myosin-II minifilaments: minifilaments assemble by three successive dimerization steps. *J. Cell Biol.* 109:1537-1547.

Somlyo, A. V., T. M. Butler, M. Bond, and A. P. Somlyo. 1981. Myosin fila-

ments have non-phosphorylated light chains in relaxed smooth muscle. *Nature (Lond.).* 294:567-569.

Suzuki, H., H. Onishi, K. Takahashi, and S. Watanabe. 1978. Structure and function of chicken gizzard myosin. *J. Biochem. (Tokyo).* 84:1529-1542.

Svitkina, T. M., A. A. Shevelev, A. D. Bershadsky, and V. I. Gelfand. 1984. Cytoskeleton of mouse embryo fibroblasts. Electron microscopy of platinum replicas. *Eur. J. Cell Biol.* 34:64-74.

Svitkina, T. M., I. G. Surgucheva, A. B. Verkhovsky, V. I. Gelfand, M. Moeremans, and J. DeMey. 1989. Direct visualization of myosin bipolar filaments in stress fibers of cultured fibroblasts. *Cell Motil. Cytoskeleton.* 12:150-156.

Toyoshima, Y. Y., C. Toyoshima, and J. A. Spudich. 1989. Bidirectional movement of actin filaments along tracks of myosin heads. *Nature (Lond.).* 341:154-156.

Trybus, K. M. 1991. Assembly of cytoplasmic and smooth muscle myosins. *Curr. Opin. Cell Biol.* 3:105-111.

Trybus, K. M., and S. Lowey. 1985. Mechanism of smooth muscle myosin phosphorylation. *J. Biol. Chem.* 260:15988-15995.

Trybus, K. M., and S. Lowey. 1987 Assembly of smooth muscle myosin minifilaments: effects of phosphorylation and nucleotide binding. *J. Cell Biol.* 105:3007-3019.

Vasiliev, J. M., and I. M. Gelfand. 1976. Effects of colcemid on morphogenetic processes and locomotion of fibroblasts. *In* Cell Motility. R. Goldman, T. Pollard, and J. Rosenbaum, editors. Cold Spring Harbor Laboratory Press. Cold Spring Harbor, New York. 279-304.

Verkhovsky, A. B., I. G. Surgucheva, T. M. Svitkina, I. S. Tint, and V. I. Gelfand. 1987. Organization of stress fibers in cultured fibroblasts after extraction of actin with bovine brain gelsolin-like protein. *Exp. Cell Res.* 173:244-255.

Weber, K., and U. Groeschel-Stewart. 1974. Antibody to myosin—the specific visualization of myosin-containing filaments in non-muscle cells. *Proc. Natl. Acad. Sci. USA.* 71:4561-4564.

Wessels, D., D. Soll, D. Knecht, W. F. Loomis, J. De Lozanne, and J. Spudich. 1988. Cell motility and chemotaxis in *Dictyostelium* amoebae lacking myosin heavy chain. *Dev. Biol.* 128:164-177.

Yumura, S., and Y. Fukui. 1985. Reversible cyclic AMP-dependent change in distribution of myosin thick filaments in Dictyostelium. *Nature (Lond.).* 314:194-196.

Zigmond, S. H., J. J. Otto, and J. Bryan. 1979. Organization of myosin in a submembranous sheath in well-spread human fibroblasts. *Exp. Cell Res.* 119:205-219.